

# Synthesis, characterization, spectral, thermal analysis and biological activity studies of some montelukast sodium complexes

Ali AE, Elasala GS, Ibrahim RS and Kolkaila AS\*

Department of Chemistry, Faculty of Science,  
Damanhour University, Damanhour, Egypt

Corresponding author: yerimabi@yahoo.com

Received on: 12/06/2021

Accepted on: 26/06/2021

Published on: 30/06/2021

## ABSTRACT

**Aim:** This study was aimed to synthesis, characterization, spectral, thermal analysis and biological activity studies of montelukast sodium and its metal complexes.

**Method and Materials:** Chromium, iron, nickel, copper, zinc, cadmium and mercury complexes were proposed to be with octahedral geometry, while manganese and cobalt complexes were with tetrahedral geometry. The thermal properties of the complexes were examined.

**Results:** The kinetic and thermodynamic parameters were estimated from the TGA and DTA curves. The thermal decomposition of the complexes ended with the formation of metal oxide as a final product except in case of Hg complex. Montelukast sodium complexes show higher biological activity than free ligand for some strains.

**Conclusion:** It was concluded that synthesis, characterization, spectral, thermal analysis and biological activity of montelukast sodium and its metal complexes were found favorable and effective.

**Keywords:** Biological activity, complexes, montelukast sodium, spectral, synthesis and thermal analysis.

**How to cite this article:** Ali AE, Elasala GS, Ibrahim RS and Kolkaila AS (2021). Synthesis, characterization, spectral, thermal analysis and biological activity studies of some montelukast sodium complexes. J. Chem. Res. Adv., 02(01): 26-41.

## Introduction

Montelukast sodium (MSod), is the orally bioavailable monosodium salt of montelukast with IUPAC name, 1-[[[(1R)-1-[3-[(1E)-2-(7-chloro-2-quinolinyl) ethenyl]phenyl-3-[2-(1-hydroxy-1-methylethyl) phenyl] propyl thio]methyl]cyclo propane acetic acid monosodium salt]. MSod is sodium salt of montelukast as drugs are often chemically made into their salt forms to enhance how the drug dissolves and to facilitate its absorption into the bloodstream. MSod has molecular formula (C<sub>35</sub>H<sub>35</sub>ClNNaO<sub>3</sub>S), molecular weight equal 608.18 g/mol is one of large number of quinoline derivatives (Peters-Golden and Henderson, 2007, Al Saadi et al., 2011 and Storms, 2007).

It is classified as leukotriene inhibitor drug that is marketed under trade names such as singular and montair, also known as (MK-0476).

MSod is selective, competitive leukotriene-receptor antagonist that selectively and competitively blocks the cysteinyl leukotriene 1 (CysLT1) receptor, preventing binding of the inflammatory mediator leukotriene D<sub>4</sub> (LTD<sub>4</sub>). MSod inhibits bronchoconstriction induced by exposure to known precipitating factors (e.g., allergens, cold and/or dry air, exercise, PAF, SO<sub>2</sub>, Aspirin) where PAF is (paroxysmal atrial fibrillation). MSod inhibits both the acute broncho constrictor response and the delayed inflammatory response to inhaled antigen (Austen, 2008, Matsuse and Kohno, 2014 and Wei et al., 2018). MSod has great role in management and treatment of bronchial asthma as it is classified as one of the most important anti-asthma drugs.

Montelukast sodium (MSod) is white to off-white in color, hygroscopic (darkens on exposure to light), found in powder form, optically active, freely soluble in ethanol, methanol, water and practically insoluble in acetonitrile. MSod is a light sensitive compound and this necessitates special handling precautions to protect it from light, in solution and in its solid state (Hoang et al., 2002, Radhakrishna et al., 2003 and AlOmari et al., 2007),

**Copyright:** Yerima and Idi. Open Access. This article is distributed under the terms of the Creative Commons Attribution 4.0 International License (<http://creativecommons.org/licenses/by/4.0/>), which permits unrestricted use, distribution, and reproduction in any medium, provided you give appropriate credit to the original author(s) and the source, provide a link to the Creative Commons license, and indicate if changes were made.

so the use of amber glass vials was required for storage the samples and also samples were wrapped with aluminum foil and protected from light, working under neon or sodium light was found to be a suitable environment this for solid samples, on the other hand MSod solutions are stable in 70% methanol and 0.1 M NaOH (Al-Omari et al., 2007 and Okumu et al., 2008).

The coordination of montelukast sodium with metal occurs through the nitrogen atom of the quinoline ring and the oxygen atom of the carboxylate group were involved in chelation. The main interest of the article was to study the synthesis, characterization, spectral, thermal analysis and biological activity studies of montelukast sodium and its metal complexes.

## Materials and Methods

### Experimental

The synthesis procedure of montelukast sodium metal complexes was carried out using hot solution of 70% methanol for both montelukast sodium and hydrated inorganic metal salt [Cr (III), Mn(II), Fe(III), Co(II), Ni(II), Cu(II), Zn(II), Cd(II) and Hg(II)] as chlorides were prepared separately. The molar amount of the metal chloride salt was mixed with the calculated amount of the ligand using mole ratios (M:L) viz. 1:1, 1:2, 1:3 and 2:1 in which (20 ml) of montelukast sodium solution in hot 70% methanol was added to (30 ml) solution of hydrated metal in hot solution of 70% methanol. In each case the reaction mixture was refluxed for about 30 min then left over-night, where the precipitated complexes were separated by filtration, then washed several times with ethanol and dried in a vacuum desiccator over anhydrous  $\text{CaCl}_2$ . Physical measurements, analytical and spectral data of the complexes are given (Tables 1 and 2).

### Measurements

Metal contents were determined by atomic absorption spectrophotometer. Carbon, hydrogen, sulphur and nitrogen analysis of montelukast sodium and all complexes recorded on CHNS Nr.11042023, at central lab, Cairo University contents of all the synthesized complexes were analyzed by the usual method (Matejovic, 1993). The analysis of chloride contents of the complexes were determined by applying the familiar Volhard method in acidic medium (Vogel, 1989). The infrared spectra of the montelukast sodium and their metal complexes recorded using Perkin

Elmer spectrophotometer, Model 1430 covering frequency range of 200-4000  $\text{cm}^{-1}$ .

Electronic spectra of the colored complexes was detected in nujol mull spectra following the method described by Lee, Griswold and Kleinberg (Lee et al., 1964) using Helios  $\alpha$  thermospectronic UVA, Mini Sipper Compatible, made in England covering the wave length range 200-1000 nm. Magnetic susceptibilities, corrected for diamagnetism using Pascal's constants were determined at room temperature (298 °K) using Faraday's method. The instrument (Rani et al., 1994) was calibrated with  $\text{Hg}[\text{Co}(\text{SCN})_4]$ . X-band electron spin resonance spectra were recorded with a reflection spectrometer operating at (9.1-9.8) GHz in a cylindrical resonance cavity with 100 KHZ modulation. The g values were determined by comparison with (2,2-diphenyl picrylhydrazide) DPPH signal ( $g=2.0037$ ) (Reinen and Friebel, 1984). Differential thermal analysis (DTA) and thermogravimetric analysis (TG) of montelukast sodium and its complexes were carried out using (Shimadzu DTA/TGA-60). The rate of heating was 10 °C/min. The cell used was platinum and the atmospheric nitrogen rate flow was 15 ml/min. The antimicrobial activities of the montelukast sodium and its complexes were examined by using (Agar well diffusion method). The bacterial indicators were: *Staphylococcus aureus* (ATCC 6538P), *Bacillus subtilis* (ATCC 19659); (Gram positive), *Escherichia Coli* (ATCC 8739) strain (Kerkeni et al., 2007) and *Pseudomonas aeruginosa* (ATCC 9027); (Gram negative) and one fungal species *Candida albicans* (ATCC 2091).

## Results and discussion

### Infrared spectral studies of montelukast sodium and its complexes:

The fundamental infrared bands of montelukast sodium and its complexes were given (Table 2 and Fig 2 & 3).

IR spectrum of the free montelukast sodium has exhibited its major bands at 3397  $\text{cm}^{-1}$  for (O-H) stretching band indicating overlapping of the peaks due to the (C-H) structure of aryl group and (C-H) stretching of methyl group peaks have appeared as shoulders between 2926  $\text{cm}^{-1}$  to 2976  $\text{cm}^{-1}$ . The (C=O) peak corresponding to (COO<sup>-</sup>) has appeared at 1636  $\text{cm}^{-1}$  along with a merged peak at 1601  $\text{cm}^{-1}$ , there is a band at 1560  $\text{cm}^{-1}$  corresponding to (C=N) of the quinoline ring, broad band at 1138  $\text{cm}^{-1}$  corresponding to (C-N), band at 1067  $\text{cm}^{-1}$  corresponding to aromatic (C-Cl) were observed,

two bands at  $836\text{ cm}^{-1}$  (aromatic C-H bending),  $697\text{ cm}^{-1}$  (C-S stretching).

All the prepared complexes contained water. In general, water in inorganic salts may be classified as lattice (water of hydration, uncoordinated water) or coordinated water. There is, however, no definite border line between the two types. Metronidazole complexes (Table 2) showed broad bands in the  $3384.31 - 3584.75\text{ cm}^{-1}$  region in all prepared complexes suggesting coordination with water. It seemed from the elemental analysis of the complexes and thermal analysis that all complexes contain water molecules in their structures. That was evident by  $\nu\text{OH}$ , Table (2). However, coordinated water in these complexes is indicated by the appearance of metal-oxygen bands attributable to rocking modes at  $420.22 - 495.61\text{ cm}^{-1}$  region (Nakamoto, 1986).

From IR spectra of montelukast sodium and its simple complexes represented in Figures (2,3) and Table (2) one can give the following:

Although carboxylate are derived from carboxylic acid, the lack of an (O-H) group make their spectra radically different, the carboxylate can stretch symmetrically and asymmetrically (Price and Wasson, 1974), these vibrations are referred as ( $\text{CO}_2$ ) stretches since the carbon and both oxygen involved giving two strong unique absorbance band the intensity of these peaks is due to the large dipole moment of the carbon-oxygen bonds, the asymmetric  $\text{CO}_2$  stretches generally fall ( $1650 - 1540\text{ cm}^{-1}$ ), the symmetric  $\text{CO}_2$  stretches generally fall ( $1450 - 1360\text{ cm}^{-1}$ ).

In general, the coordinated bonds are intermediate between purely ionic and purely covalent. It was reported further that there was a relationship between the covalent character of the metal-carboxylate bond and the positions of the  $\text{COO}^-$  absorptions as the difference in frequency between the asymmetric and the symmetric  $\text{COO}^-$  stretching vibrations may serve as a measure of covalency. An increase of covalent character leads to more asymmetric structure of the carboxyl group and results were in an increase in the frequency separation of the two carboxyl bands (asymmetric and symmetric).

It was expected that the covalent character of the M-OOC bond predicts stable bonding in the studied complexes. Carboxylate groups when coordinated in a complex compound are known to give rise to another peak in the ( $1450 - 1360\text{ cm}^{-1}$ ) region so in montelukast sodium free ligand IR

spectrum showed. The C=O peak corresponding to ( $\text{COO}^-$ ) has appeared at  $1636\text{ cm}^{-1}$  along with a merged peak at  $1601\text{ cm}^{-1}$ . But in the prepared MSod simple complexes IR spectra C=O band wave number shifted to lower frequency ( $1625 - 1615\text{ cm}^{-1}$ ) as asymmetric stretching band, also in complexes IR spectra there is appearance of new band at the ( $1416 - 1406\text{ cm}^{-1}$ ) range (Table 2), indicated the symmetric stretching band and showed coordination through that group.

Carboxylate ligand can bind to the metal either monodentate or bidentate, giving changes in the relative positions of the asymmetric and symmetric stretching vibrations. The IR spectra of the complexes gave a separation value of  $> 200\text{ cm}^{-1}$  suggesting monodentate carboxylate. The remaining carboxylate bands  $\gamma(\text{COO}^-)$ ,  $\rho(\text{COO}^-)$  and  $\omega(\text{COO}^-)$ , formerly at  $759.75$ ,  $619.15$  and  $528.00\text{ cm}^{-1}$  respectively showed change in position as a result of coordination.

The MSod IR spectrum shows band at ( $1560\text{ cm}^{-1}$ ) characteristic to (C=N) of the quinoline ring, in all complexes the (C=N) is shifted to lower wave numbers in the spectra ( $1537 - 1530\text{ cm}^{-1}$ ) indicating coordination through that group.

Also broad band at ( $1138\text{ cm}^{-1}$ ) corresponding to (C-N) in free ligand is shifted to higher frequency in the complexes spectra ( $1186 - 1154\text{ cm}^{-1}$ ) and this confirm that (C=N) of the quinoline ring participate in the coordination. (C-Cl) of the aromatic ring has wave number at ( $1067\text{ cm}^{-1}$ ) was shifted to higher frequency in the complexes ( $1077 - 1089\text{ cm}^{-1}$ ) which confirmed the previous postulate. C-S stretching in the MSod IR spectrum appeared at ( $697\text{ cm}^{-1}$ ) had no significant change in the prepared complexes suggesting it has no role in the coordination.

In the far IR spectra, the bonding of nitrogen and oxygen is provided by the presence of bands at ( $534 - 465\text{ cm}^{-1}$ ) (M-N) and ( $469 - 411\text{ cm}^{-1}$ ) (M-O). The metal complexes of MSod possess chloride attached to the metal ions which were supported by the presence of  $\nu(\text{M-Cl})$  at ( $377 - 346\text{ cm}^{-1}$ ).

#### *Electronic Spectra and magnetic susceptibility ( $\mu_{\text{eff}}$ ) studies*

The nujol mull electronic absorption spectrum for the bluish green chromium-complex,  $[\text{Cr}_2(\text{montelukast sodium})\text{Cl}_5(\text{H}_2\text{O})_5]\cdot\text{H}_2\text{O}$ , Table (3), gave ( $\lambda_{\text{max}}$ - nm) of the characteristic bands gathered with room temperature magnetic moment values. The nujol mull spectrum for this complex exhibited three bands at  $335$ ,  $450$ ,  $590\text{ nm}$  the first

Table 1: Elemental analysis, m.p, formula, molecular weight ,stoichiometries and colour of montelukast sodium and its complexes. All the complexes have m.p&gt; 300° C

Ligand /Complex	Color	M.wt.	Calculated/ (found)%					
			C%	H%	N%	S%	M%	Cl%
Montelukast Sodium (C <sub>35</sub> H <sub>35</sub> Cl N NaO <sub>3</sub> S)	Off-white	608.17	69.12	5.80	2.30	5.27	-----	5.83
Cr <sub>2</sub> (MSod) Cl <sub>5</sub> (H <sub>2</sub> O) <sub>5</sub> .H <sub>2</sub> O (2: 1)	Bluish green	974.51	43.14 (43.02)	4.86 (4.57)	1.44 (1.31)	3.29 (3.08)	10.67 (10.93)	21.83 (21.69)
[Mn <sub>2</sub> (MSod) Cl <sub>3</sub> (H <sub>2</sub> O) <sub>3</sub> ].H <sub>2</sub> O (2:1)	Yellow	873.47	48.13 (47.95)	4.96 (4.75)	1.60 (1.51)	3.67 (3.50)	12.58 (12.20)	16.23 (16.01)
[Fe <sub>2</sub> (MSod) Cl <sub>5</sub> (H <sub>2</sub> O) <sub>5</sub> ].H <sub>2</sub> O (2:1)	Dark Orange	982.21	42.80 (42.58)	4.82 (4.59)	1.43 (1.32)	3.26 (3.09)	11.37 (11.52)	21.66 (21.43)
[Co <sub>2</sub> (MSod) Cl <sub>3</sub> (H <sub>2</sub> O) <sub>3</sub> ].H <sub>2</sub> O (2:1)	Pink	881.46	47.69 (47.49)	4.92 (4.83)	1.59 (1.48)	3.64 (3.49)	13.37 (13.40)	16.09 (15.82)
[Ni <sub>2</sub> ( MSod) Cl <sub>3</sub> (H <sub>2</sub> O) <sub>7</sub> ].H <sub>2</sub> O (2: 1)	Pale green	953.04	44.11 (43.86)	5.39 (5.27)	1.47 (1.40)	3.36 (3.28)	12.32 (12.85)	14.88 (14.57)
[Cu <sub>2</sub> ( MSod) Cl <sub>3</sub> (H <sub>2</sub> O) <sub>7</sub> ].H <sub>2</sub> O (2: 1)	Olive green	962.74	43.67 (43.52)	5.34 (5.45)	1.45 (1.38)	3.33 (3.14)	13.20 (13.90)	14.73 (14.60)
[Zn <sub>2</sub> ( MSod) Cl <sub>3</sub> (H <sub>2</sub> O) <sub>7</sub> ].H <sub>2</sub> O (2: 1)	Yellow	966.41	43.50 (43.37)	5.32 (5.24)	1.45 (1.29)	3.32 (3.29)	13.53 (13.07)	14.67 (14.49)
[Cd <sub>2</sub> (MSod) Cl <sub>3</sub> (H <sub>2</sub> O) <sub>7</sub> ].H <sub>2</sub> O (2: 1)	Yellow	1060.47	39.64 (39.46)	4.85 (4.72)	1.32 (1.29)	3.02 (2.89)	21.20 (21.78)	13.37 (13.18)
[Hg <sub>2</sub> (MSod) Cl <sub>3</sub> (H <sub>2</sub> O) <sub>7</sub> ].H <sub>2</sub> O (2: 1)	Deep Yellow	1236.83	33.99 (33.74)	4.16 (4.01)	1.13 (1.02)	2.59 (2.43)	32.44 (32.43)	11.46 (11.29)

Table 2: Fundamental infrared bands (cm<sup>-1</sup>) of montelukast sodium (MSod) and its metal complexes.

Compound	$\nu$ O-H (H <sub>2</sub> O)	$\nu$ COO (asymm)	$\nu$ COO (symm)	$\Delta\nu$ (COO)	$\nu$ (C=N)	$\nu$ (C-N)	$\nu$ (C-Cl)	$\nu$ (C-S)	$\nu$ (M-N)	$\nu$ (M-O)	$\nu$ (M-Cl)
Montelukast sodium	-----	1636	-----	-----	1560	1138	1067	697	-----	-----	-----
[Cr <sub>2</sub> (MSod) Cl <sub>5</sub> (H <sub>2</sub> O) <sub>5</sub> ].H <sub>2</sub> O (2: 1)	3410	1625	1416	209	1538	1159	1081	695	534	466	377
[Mn <sub>2</sub> (MSod) Cl <sub>3</sub> (H <sub>2</sub> O) <sub>3</sub> ].H <sub>2</sub> O (2:1)	3418	1622	1406	216	1530	1155	1085	696	499	411	350
[Fe <sub>2</sub> (MSod) Cl <sub>5</sub> (H <sub>2</sub> O) <sub>5</sub> ].H <sub>2</sub> O (2:1)	3416	1621	1412	209	1535	1156	1081	695	493	431	346
[Co <sub>2</sub> (MSod) Cl <sub>3</sub> (H <sub>2</sub> O) <sub>3</sub> ].H <sub>2</sub> O (2:1)	3422	1615	1408	207	1532	1168	1078	697	465	411	340
[Ni <sub>2</sub> ( MSod) Cl <sub>3</sub> (H <sub>2</sub> O) <sub>7</sub> ].H <sub>2</sub> O (2: 1)	3435	1620	1410	210	1530	1154	1080	697	494	411	352
[Cu <sub>2</sub> ( MSod) Cl <sub>3</sub> (H <sub>2</sub> O) <sub>7</sub> ].H <sub>2</sub> O (2: 1)	3447	1623	1414	209	1535	1158	1081	695	539	465	372
[Zn <sub>2</sub> ( MSod) Cl <sub>3</sub> (H <sub>2</sub> O) <sub>7</sub> ].H <sub>2</sub> O (2: 1)	3449	1625	1410	215	1534	1156	1089	697	496	411	362
[Cd <sub>2</sub> (MSod) Cl <sub>3</sub> (H <sub>2</sub> O) <sub>7</sub> ].H <sub>2</sub> O (2: 1)	3539	1618	1407	211	1537	1155	1080	696	495	409	347
[Hg <sub>2</sub> (MSod) Cl <sub>3</sub> (H <sub>2</sub> O) <sub>7</sub> ].H <sub>2</sub> O (2: 1)	3525	1620	1414	206	1535	1154	1077	695	532	469	369

two was due to  ${}^4A_{2g} \rightarrow {}^4T_{2g}$  (F),  ${}^4A_{2g} \rightarrow {}^4T_{1g}$  (F) and the latter is due to  ${}^4A_{2g} \rightarrow {}^4T_{1g}$  (p) transitions. So that, the complex had octahedral geometry. Such O<sub>h</sub> geometry was further deduced from the room temperature magnetic moment value ( $\mu_{\text{eff}}$ ) for this complex which equal 7.4 B.M (Kent et al., 1968, Howlader et al., 2000 and Sreekanth et al., 2006).

The yellow electronic absorption spectrum of [Mn<sub>2</sub>(montelukast sodium) Cl<sub>3</sub>(H<sub>2</sub>O)<sub>3</sub>]. H<sub>2</sub>O,

presented three major absorptions maxima at bands 300 , 350, 420 nm .Where the first band is assigned to  ${}^6A_{1g} \rightarrow {}^4A_{1g}$  , while the second is due to  ${}^6A_{1g} \rightarrow {}^4T_{2g}$  transition and the last band is due to  ${}^6A_{1g} \rightarrow {}^4T_{1g}$  transition (Howlader et al., 2000 and Sreekanth et al., 2006). Its room temperature ( $\mu_{\text{eff}}$ ) value equals 11.8 B.M. typified the existence of tetrahedral configuration for the complex.

The electronic absorption spectrum of the

orange  $[\text{Fe}_2(\text{montelukast sodium})_3 \text{Cl}_5 \cdot (\text{H}_2\text{O})_5]$ .  $\text{H}_2\text{O}$  present three major absorptions maxima at 320, 375, 450 nm respectively. These bands are due to CT ( $t_{2g} \rightarrow \pi^*$ ) and CT ( $\pi \rightarrow e_g$ ). So that, the complex has  $O_h$  geometries. Such octahedral (Grau et al., 2013 and Barnum, 1961) was further deduced from the  $\mu_{\text{eff}}$  values which equals, 11.6 B.M.

The nujol mull electronic absorption spectral bands of the pink  $[\text{Co}_2(\text{montelukast sodium})\text{Cl}_3 \cdot (\text{H}_2\text{O})_3] \cdot \text{H}_2\text{O}$  complexes gave bands at 340, 430, 665. The first two bands complex were of metal to ligand charge transfer nature and the latter broad band in the spectrum for Co-montelukast sodium complex was assigned to  ${}^4A_2(F) \rightarrow {}^4T_1(P)$  transition indicating the tetrahedral structure (Carlin and Baker, 1964, Jorgensen, 1962 and Masoud et al., 2007) with  $\mu_{\text{eff}} = 7.8$  B.M. which verified such geometry.

The nujol mull electronic spectrum of the pale green nickel-complex,  $[\text{Ni}_2(\text{montelukast sodium})\text{Cl}_3(\text{H}_2\text{O})_7] \cdot \text{H}_2\text{O}$  present three major absorptions maxima 340, 420, 685 nm. The first two bands are taken as assignable to  ${}^3A_2(g) \rightarrow {}^3T_1(g)$  and the latter broad band is due to  ${}^3A_2(g) \rightarrow {}^3T_1(g)$  transitions. The broadness is attributed to the existence of more than d-d transition overlapped with each other (Lever, (1968). So that, complex has  $O_h$  geometries, such octahedral was further deduced from the  $\mu_{\text{eff}}$  values which equals (5.4) B.M.

The olive green  $[\text{Cu}_2(\text{montelukast sodium})\text{Cl}_3(\text{H}_2\text{O})_7] \cdot \text{H}_2\text{O}$  exhibited bands at 334, 435, 745 nm. The latter broad band was assigned to the transition  ${}^2E_g \rightarrow {}^2T_{2g}(D)$  transition assignable to octahedral environment, such octahedral was further deduced from the  $\mu_{\text{eff}}$  value which equals (3.1) B.M.

The nujol mull electronic spectra of the Zn, Cd and Hg complexes exhibited only a high intensity band at 329-365 nm, which are assigned to ligand  $\rightarrow$  metal charge transfer. Owing to the  $d^{10}$ -configuration of Zn(II), Cd(II) and Hg(II), no d-d transition could be observed and therefore the stereochemistry around these metals in their complexes cannot be determined from ultraviolet and visible spectra. However, by comparing the spectra of these complexes and those of similar environments, octahedral and tetrahedral geometries are suggested for these complexes (Masoud et al., 2015a,b and Masoud et al., 2013). These complexes were diamagnetic ( $\mu_{\text{eff}} = \text{zero}$ ).

#### *Electron spin resonance (ESR) for copper complex:*

The room temperature poly crystalline X-band ESR spectral pattern of the rhombic olive green copper montelukast sodium complex with the formula,  $[\text{Cu}_2(\text{MSod})\text{Cl}_3(\text{H}_2\text{O})_7] \cdot \text{H}_2\text{O}$  gauss (Fig 5 & Table 4) gave three peaks at 3000, 3100 and 3300 gauss values with  $g_1$ ,  $g_2$  and  $g_3$  tensor values 2.219, 2.147 and 2.017 respectively, i.e. the trend is  $g_1 > g_2 > g_3$ .

The calculated  $g_{\text{av}}$  value (2.128) is obtained from the following equation:

$$g_{\text{av}} = 1/3 (g_1 + g_2 + g_3)$$

R was calculated from the relation (Condon, 1928) :  $R = (g_2 - g_1) / (g_3 - g_2)$ . If R is  $>1$ , a predominantly  $d_{z^2}$  ground state is present with trigonalbipyramidal geometry (TBP), while with  $R < 1$ , the ground state should be  $d_{x^2-y^2}$  of square pyramidal (SPY) geometry (Masoud et al., 1998), if  $R = 1$  then the ground state is approximately an equal mixture of  $d_{z^2}$  and  $d_{x^2-y^2}$ . For this complex the (R) value = 0.55 (Table 4), typified the existence of (SPY) geometry of  $d_{x^2-y^2}$  ground state.

#### *Electron spin resonance of cobalt complexes*

Degeneracy of the 'd' orbitals will be resolved when metal ion is placed in crystal field by the electrostatic interaction which means the crystal removal of the orbital degeneracy. However, the resolve of degeneracy for more than one unpaired electron is present (even number of unpaired electron) through zero field splitting phenomenon, but one unpaired electron spin degeneracy can only be removed by magnetic field (Boca, 2004).

Magnetic resonance can also occur without an external magnetic field from interaction of the electron and nuclear spin. Fine and hyperfine structure (Abragam and Pryce, 1951) of atomic spectra was produced by such resonance. The nuclei in molecule or complex often have magnetic moment which produce local magnetic field at the electron, the interaction between an unpaired electron and the nuclei with non-zero nuclear spin is called the hyperfine interaction, this lead to splitting of ESR line and is known as hyperfine splitting.

When the species contain an odd number of unpaired electron like  $\text{Co}^{2+}$  ( $d^7$ ), so Kramer degeneracy (Canadas et al., 2000 and Aasa, 1970) must exist and so the zero field splitting produce two doubly degenerate spin states ( $m_s = \pm 3/2, \pm 1/2$ ) each of these levels was splitted in to singlet by the applied magnetic field producing four levels with three ESR peaks, this spectrum was further complicated due to the cobalt nucleus with

Table (3): Nujol mull electronic absorption spectra  $\lambda_{\max}$  (nm), room temperature effective magnetic moment values ( $\mu_{\text{eff}}$ 298°K) and geometries of montelukast sodium (MSod) metal complexes

Complex	Color	Absorption region (nm) ( $\lambda_m$ )	Band assignment	Magnetic moment $\mu_{\text{eff}}$ (B.M)	Geometry
[Cr <sub>2</sub> (MSod) Cl <sub>5</sub> (H <sub>2</sub> O) <sub>5</sub> ].H <sub>2</sub> O (2: 1)	Bluish green	335 450 590	<sup>4</sup> A <sub>2g</sub> → <sup>4</sup> T <sub>2g</sub> (F) <sup>4</sup> A <sub>2g</sub> → <sup>4</sup> T <sub>1g</sub> (F) <sup>4</sup> A <sub>2g</sub> → <sup>4</sup> T <sub>1g</sub> (P)	7.4	O <sub>h</sub>
[Mn <sub>2</sub> (MSod) Cl <sub>3</sub> (H <sub>2</sub> O) <sub>3</sub> ].H <sub>2</sub> O (2:1)	Yellow	300 350 420	<sup>6</sup> A <sub>1</sub> → <sup>4</sup> A <sub>1</sub> <sup>6</sup> A <sub>1</sub> → <sup>4</sup> T <sub>2</sub> <sup>6</sup> A <sub>1</sub> → <sup>4</sup> T <sub>1</sub>	11.8	T <sub>d</sub>
[Fe <sub>2</sub> (MSod) Cl <sub>5</sub> (H <sub>2</sub> O) <sub>5</sub> ].H <sub>2</sub> O (2:1)	Orange	320 375 450	CT (t <sub>2g</sub> →π*) CT (π→e <sub>g</sub> ).	11.6	O <sub>h</sub>
[Co <sub>2</sub> (MSod) Cl <sub>3</sub> (H <sub>2</sub> O) <sub>3</sub> ].H <sub>2</sub> O (2:1)	Pink	340 430 665	CT CT <sup>4</sup> A <sub>2</sub> (F)→ <sup>4</sup> T <sub>1</sub> (P)	7.8	T <sub>d</sub>
[Ni <sub>2</sub> (MSod) Cl <sub>3</sub> (H <sub>2</sub> O) <sub>7</sub> ].H <sub>2</sub> O (2: 1)	Pale green	340, 420 685	<sup>3</sup> A <sub>2g</sub> (F)→ <sup>3</sup> T <sub>1g</sub> (F) <sup>3</sup> A <sub>2g</sub> (F)→ <sup>3</sup> T <sub>1g</sub> (P)	5.4	O <sub>h</sub>
[Cu <sub>2</sub> (MSod) Cl <sub>3</sub> (H <sub>2</sub> O) <sub>7</sub> ].H <sub>2</sub> O (2: 1)	Olive green	334, 435 745	<sup>2</sup> E <sub>g</sub> → <sup>2</sup> T <sub>2g</sub> (D)	3.1	O <sub>h</sub>
[Zn <sub>2</sub> (MSod) Cl <sub>3</sub> (H <sub>2</sub> O) <sub>7</sub> ].H <sub>2</sub> O (2: 1)	yellow	355,425	CT	Zero	O <sub>h</sub>
[Cd <sub>2</sub> (MSod) Cl <sub>3</sub> (H <sub>2</sub> O) <sub>7</sub> ].H <sub>2</sub> O (2: 1)	yellow	335,440	CT	Zero	O <sub>h</sub>
[Hg <sub>2</sub> (MSod) Cl <sub>3</sub> (H <sub>2</sub> O) <sub>7</sub> ].H <sub>2</sub> O (2: 1)	yellow	305,350,440	CT	Zero	O <sub>h</sub>

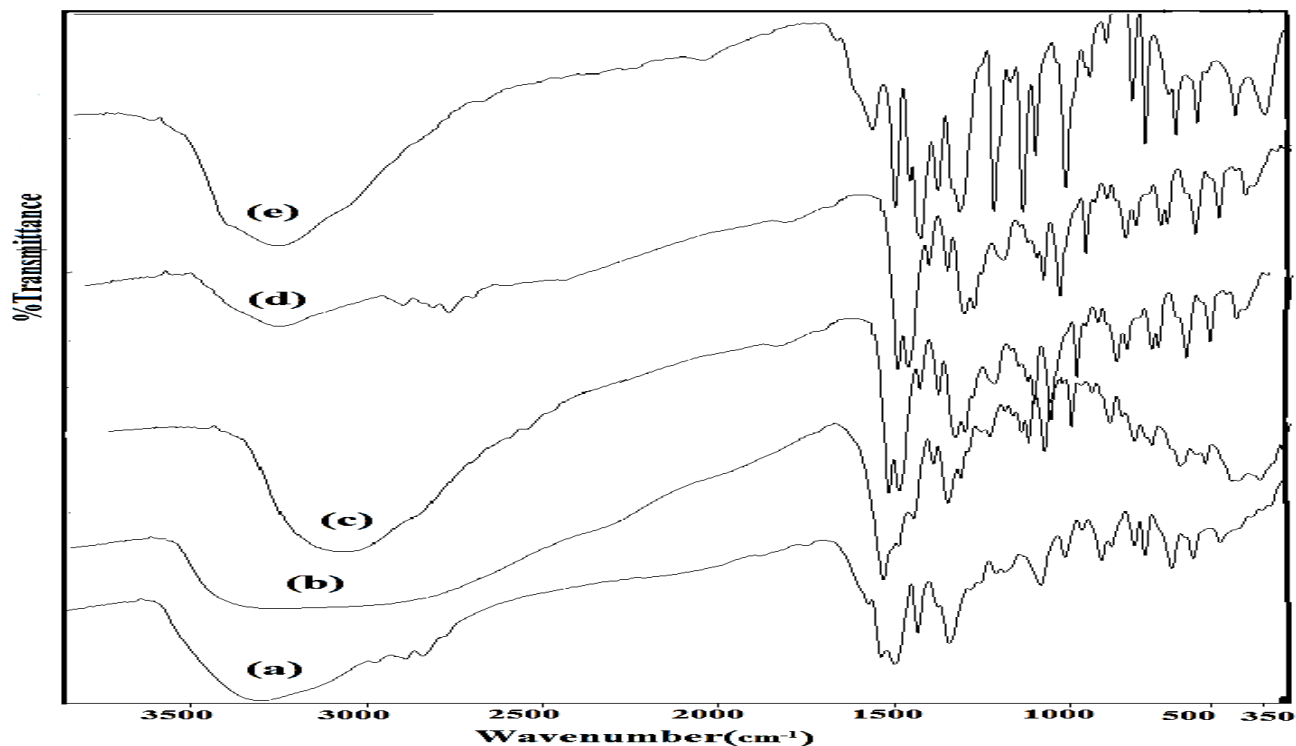


Fig 2: Infrared bands of montelukast sodium and its metal complexes.

- (a):Montelukast sodium  
 (b): [Cr<sub>2</sub>(MSod) Cl<sub>5</sub>(H<sub>2</sub>O)<sub>5</sub>].H<sub>2</sub>O  
 (c): [Mn<sub>2</sub>(MSod) Cl<sub>3</sub>(H<sub>2</sub>O)<sub>3</sub>].H<sub>2</sub>O  
 (d):[Fe<sub>2</sub>(MSod) Cl<sub>5</sub>(H<sub>2</sub>O)<sub>5</sub>].H<sub>2</sub>O  
 (e) :[Co<sub>2</sub>(MSod) Cl<sub>3</sub>(H<sub>2</sub>O)<sub>3</sub>].H<sub>2</sub>O

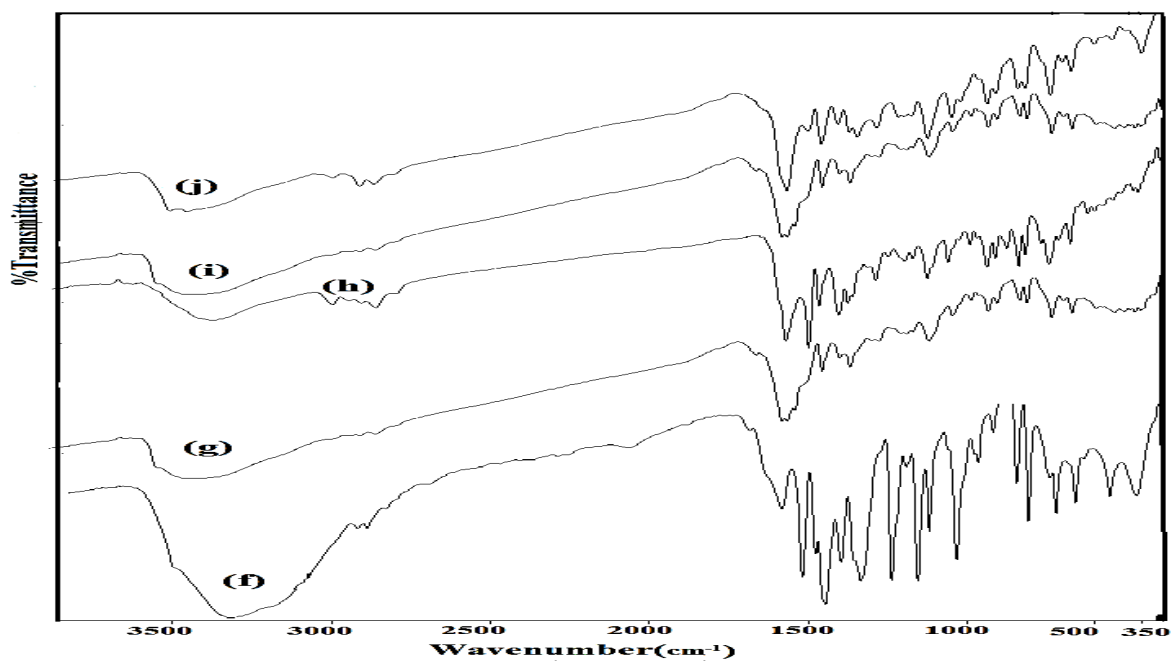


Fig 3: Infrared bands of some montelukast sodium metal complexes.

- (f):  $[\text{Ni}_2(\text{MSod})\text{Cl}_3(\text{H}_2\text{O})_7]\cdot\text{H}_2\text{O}$   
 (g):  $[\text{Cu}_2(\text{MSod})\text{Cl}_3(\text{H}_2\text{O})_7]\cdot\text{H}_2\text{O}$   
 (h):  $[\text{Zn}_2(\text{MSod})\text{Cl}_3(\text{H}_2\text{O})_7]\cdot\text{H}_2\text{O}$   
 (i):  $[\text{Cd}_2(\text{MSod})\text{Cl}_3(\text{H}_2\text{O})_7]\cdot\text{H}_2\text{O}$   
 (j):  $[\text{Hg}_2(\text{MSod})\text{Cl}_3(\text{H}_2\text{O})_7]\cdot\text{H}_2\text{O}$

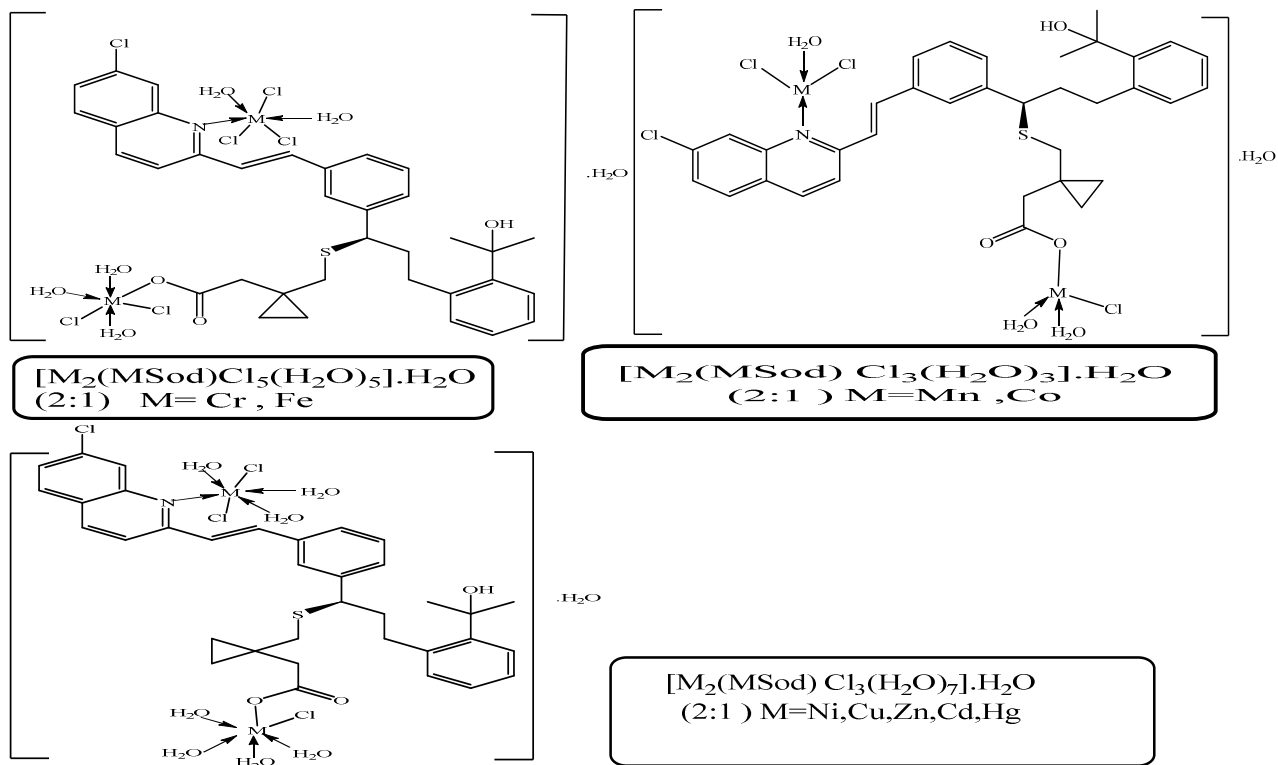


Fig 4: Proposed structure of montelukast sodium metal complexes

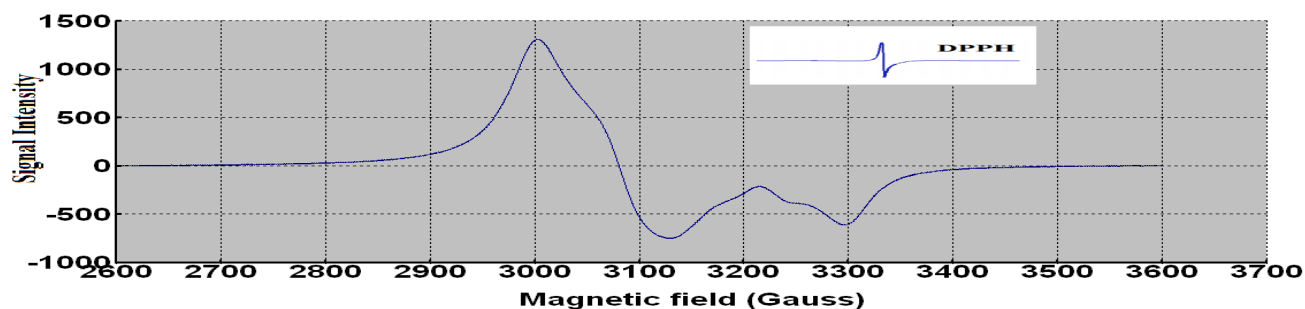
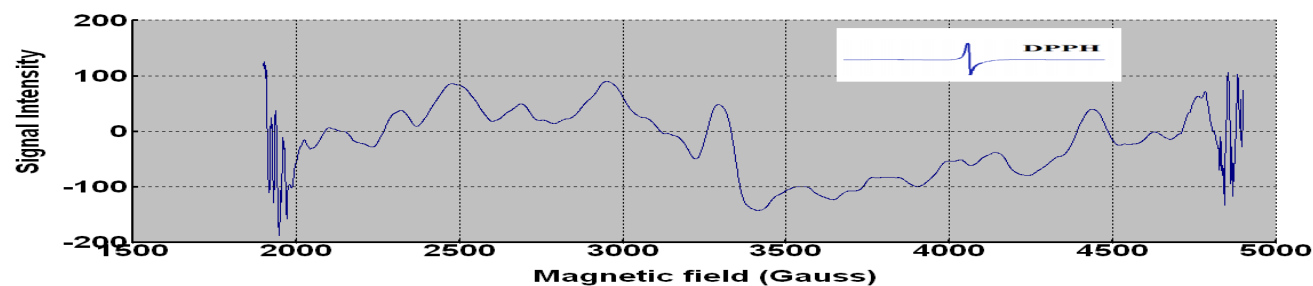
Fig 5: ESR spectrum for  $[\text{Cu}_2(\text{MSod})\text{Cl}_3(\text{H}_2\text{O})_7]\cdot\text{H}_2\text{O}$  complex.Fig 6 : ESR spectrum for  $[\text{Co}_2(\text{MSod}) \text{Cl}_3(\text{H}_2\text{O})_3]\cdot\text{H}_2\text{O}$  complex.

Table 4: Room temperature ESR spectral parameters of copper montelukast sodium complex.

Complex	$g_1$	$g_2$	$g_3$	$\langle g \rangle$	$A_1 \cdot 10^{-4}$	$A_2 \cdot 10^{-4}$	$A_3 \cdot 10^{-4}$	R
Cu-MSod complex	2.219	2.147	2.017	2.128	122	66.66	238	0.55

Table 5: The antifungal activity of the montelukast sodium and its complexes against some reference strains expressed in absolute activity (AU)

Compound (Cpd)	<i>Staphylococcus aureus</i>		<i>Bacillus subtilis</i>		<i>Pseudomonas aeruginosa</i>		<i>Escherichia coli</i>		<i>Candida albicans</i>	
	Demso	Cpd.	Demso	Cpd.	Demso	Cpd.	Demso	Cpd.	Demso	Cpd.
Montelukast Sodium	8	10	8	10	8	8	8	8	8	8
$[\text{Cu}_2(\text{MSod})\text{Cl}_3(\text{H}_2\text{O})_7]\cdot\text{H}_2\text{O}$	8	14	8	15	8	17	8	12	8	12
$[\text{Zn}_2(\text{MSod})\text{Cl}_3(\text{H}_2\text{O})_7]\cdot\text{H}_2\text{O}$	8	12	8	15	8	8	8	8	8	13
Ciprofloxacin	9	30	9	30	9	30	9	30	-	-
Clotrimazole	-	-	-	-	-	-	-	-	10	17

nuclear spin (Lines, 1971) ( $I = 7/2$ ) which cause the absorption signal to be split in to  $(2nI+1)$  (Abragam A and Pryce, 1951) where (n) was the number of nucleus, So presence of eight peaks in ESR spectrum of Co-MSod was result of coming in vicinity to the nucleus ( $2 \cdot 1 \cdot 7/2 + 1 = 8$ , as found (Fig 6).

#### Biological activity:

Five microorganisms representing different microbial categories, Gram positive (*Staphylococcus aureus* (ATCC 6538P), *Bacillus subtilis* (ATCC 19659)), Gram negative (*Escherichia coli* (ATCC 8739) strain and *Pseudomonas aeruginosa* (ATCC 9027)) and one fungal species (*Candida albicans* (ATCC 2091)).

Montelukast sodium showed activity to gram positive (*Staphylococcus aureus*, *Bacillus subtilis*), with inhibition zone equal 10 for both and showed lower activity towards Gram negative (*Escherichia coli* strain and *Pseudomonas aeruginosa*) and *Candida albicans* with inhibition zone equal 8.

$[\text{Cu}_2(\text{MSod}) \text{Cl}_3(\text{H}_2\text{O})_7]\cdot\text{H}_2\text{O}$  complex showed higher activity to *Pseudomonas aeruginosa*, *Bacillus subtilis* and *Staphylococcus aureus*. It revealed by the diameter of its inhibition zone which equal 17,15 and 14 respectively. It showed activity in the same range for both *Escherichia coli* and *Candida albicans* with inhibition zone equal 12 for both.

$[\text{Zn}_2(\text{MSod}) \text{Cl}_3(\text{H}_2\text{O})_7]\cdot\text{H}_2\text{O}$  complex showed higher activity to *Candida albicans*, *Bacillus subtilis*





The DTA data of  $[\text{Co}_2(\text{MSod}) \text{Cl}_3(\text{H}_2\text{O})_3] \cdot \text{H}_2\text{O}$  complex, (Fig 8 and Table 6), gave three peaks at 367.9, 603 and 736.6K with activation energies of 17.95, 47.45 and 93.70 kJ/mole and their orders are 1.50, 1.40 and 1.38, respectively. All peaks are exothermic except the first one is endothermic in nature. All the peaks are of the first order type except the first one is of the second order. The mechanism of decomposition could be represented in the following scheme (2):

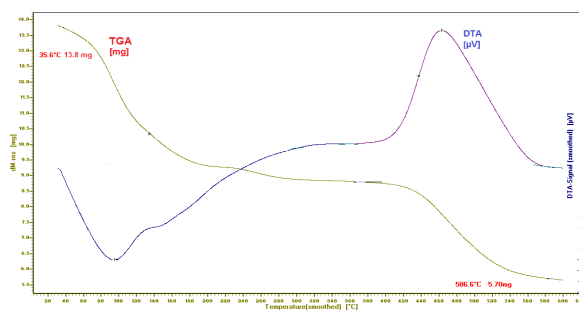
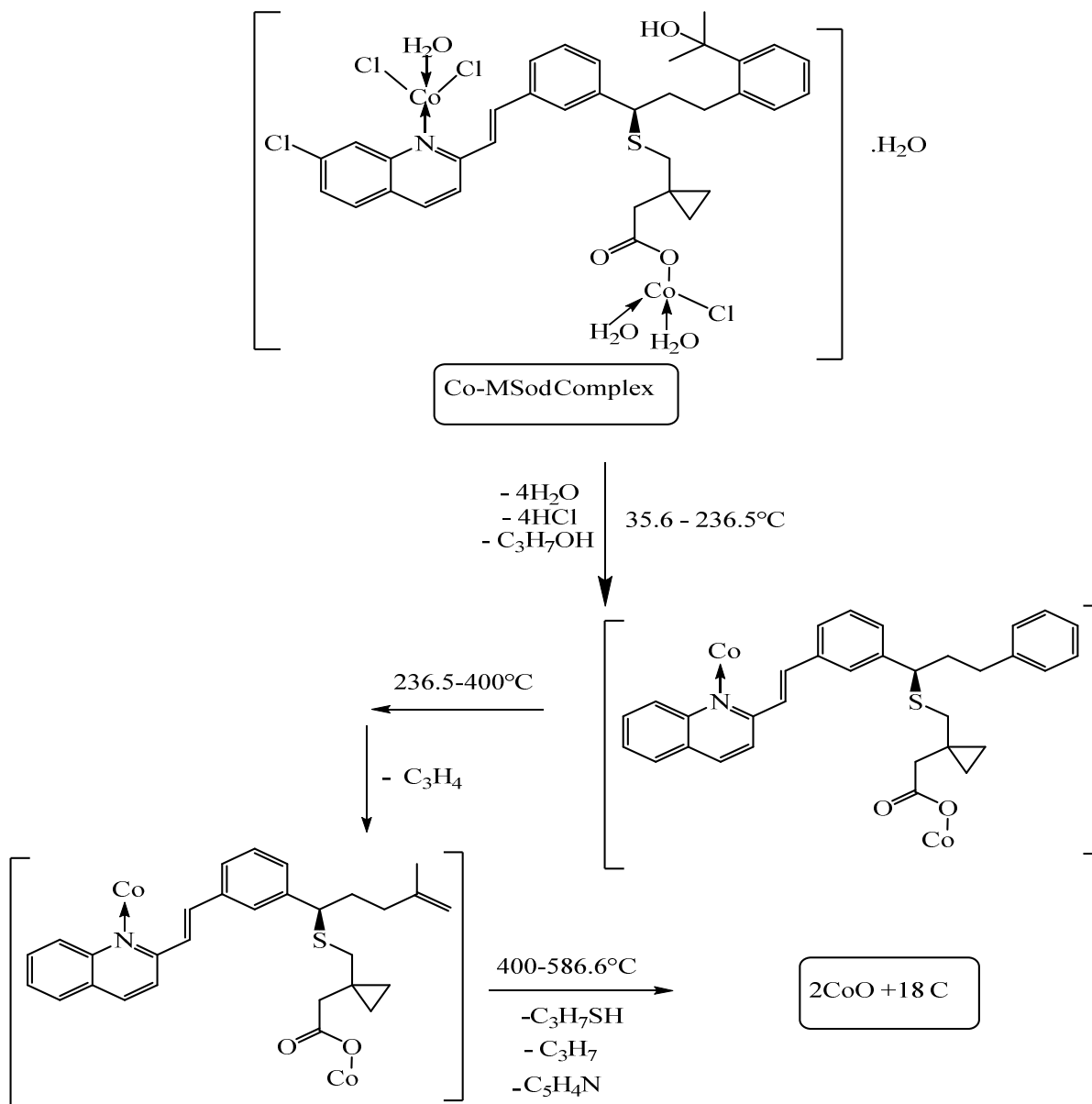


Fig 8: TGA and DTA curves of  $[\text{Co}_2(\text{MSod}) \text{Cl}_3(\text{H}_2\text{O})_3] \cdot \text{H}_2\text{O}$  complex.



Scheme 2: Thermolysis of  $[\text{Co}_2(\text{MSod}) \text{Cl}_3(\text{H}_2\text{O})_3] \cdot \text{H}_2\text{O}$  Complex.

However, the thermolysis of  $[\text{Cu}_2(\text{MSod})\text{Cl}_3(\text{H}_2\text{O})_7]\cdot\text{H}_2\text{O}$  complex, (Fig 9 and Table 6), showed well defined two peaks at 392.9 and 685.6K with activation energies 18.60 and 37.87 kJ/mole, respectively. The orders of reactions were 1.56 and 1.43, respectively. The second peak is of exothermic types while the first peak is endothermic type. The first peak is of the second order type and the first peak is first order type. The mechanism of decomposition could be represented in the following scheme (3):

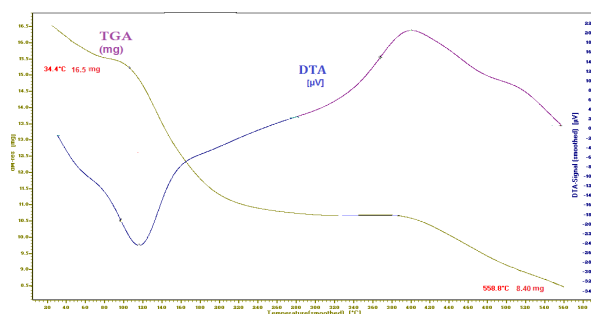
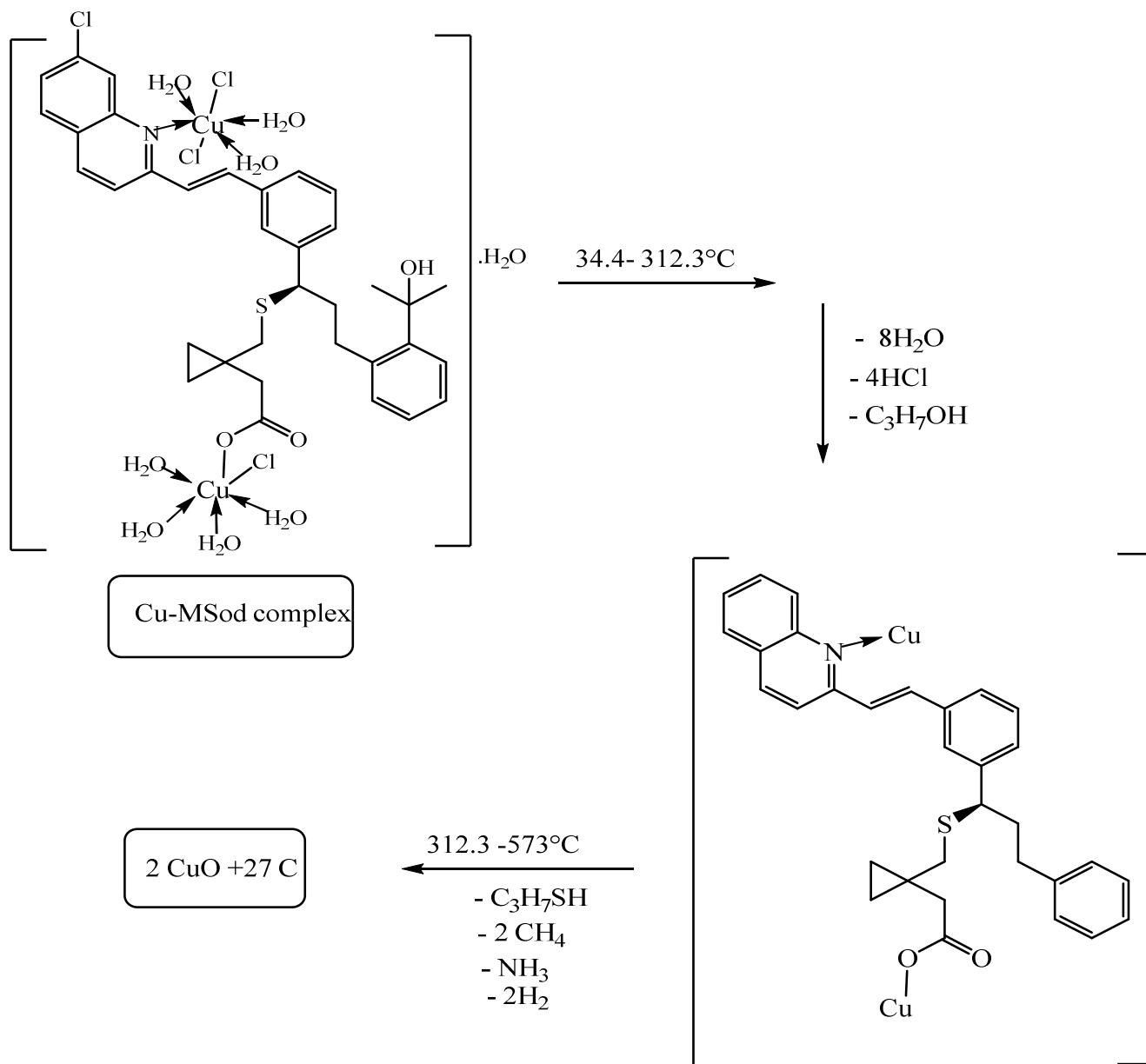


Fig 9: TGA and DTA curves of  $[\text{Cu}_2(\text{MSod})\text{Cl}_3(\text{H}_2\text{O})_7]\cdot\text{H}_2\text{O}$  complex.



**Scheme 3:** Thermolysis of  $[\text{Cu}_2(\text{MSod})\text{Cl}_3(\text{H}_2\text{O})_7]\cdot\text{H}_2\text{O}$  Complex.

The thermal sheet of  $[\text{Hg}_2(\text{MSod})\text{Cl}_3(\text{H}_2\text{O})_7]\cdot\text{H}_2\text{O}$  complex, Figure (10) and Table (6), gave a well-defined three peaks. The first one is endothermic while the last two peaks are exothermic at 379.5, 645 and 760.9 K with activation energies of 13.19, 66.35 and 98.23 kJ/mole and their orders are 1.61, 1.28 and 1.31. All peaks are of the first order type except the first peak is second order type. The two last peaks in DTA overlapped to give one step in TGA, sublimation of mercury occurred and no metal oxide formed as residue. The mechanism of decomposition could be represented in the following scheme (4):

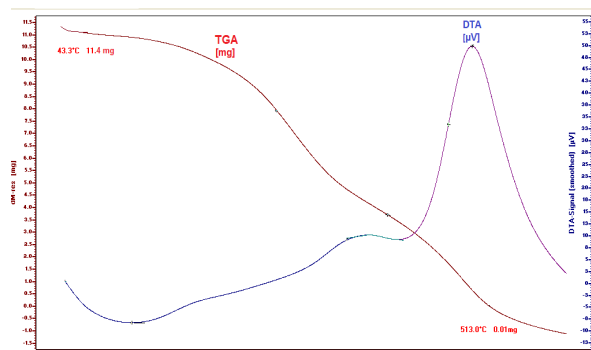
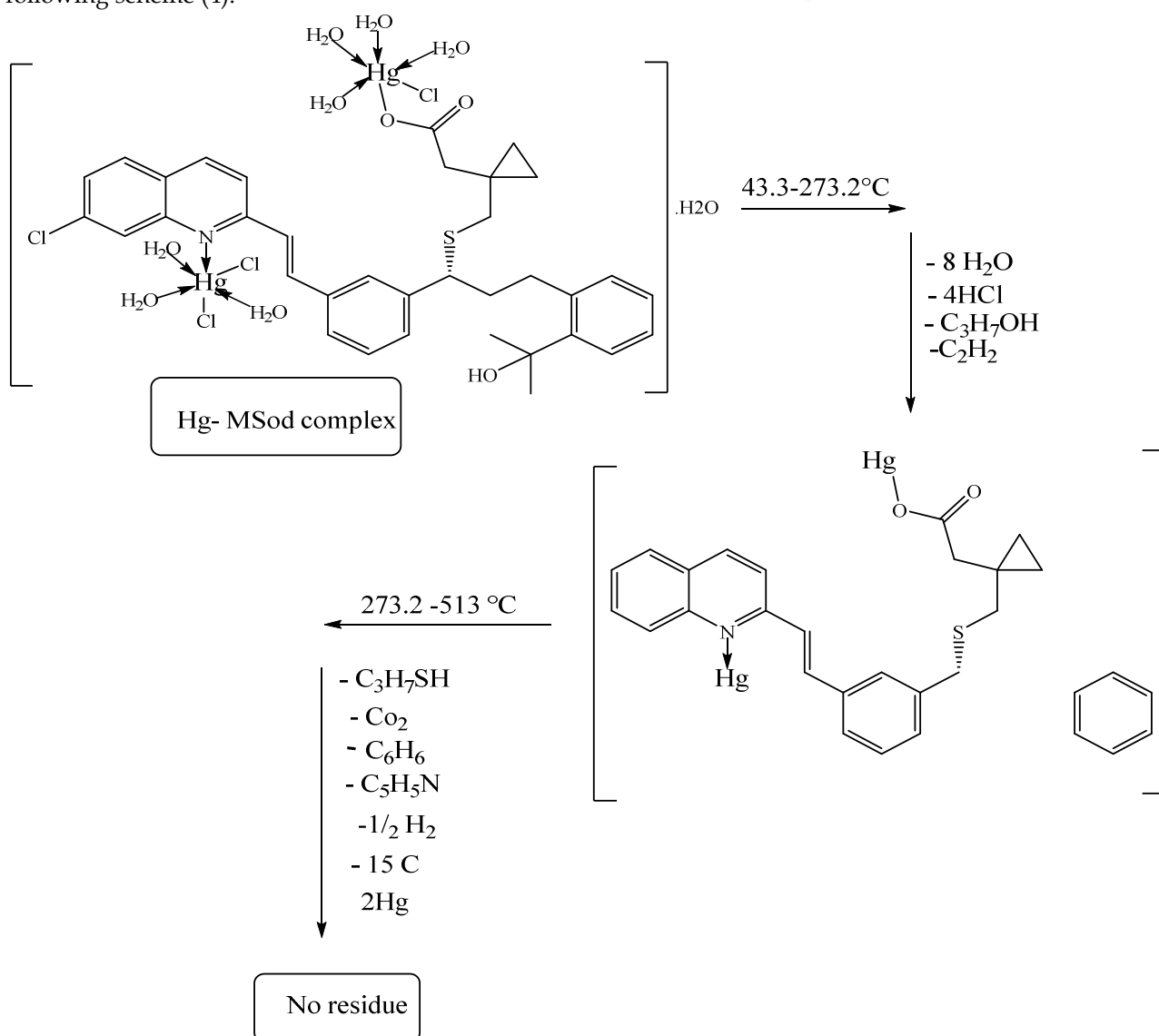


Fig 10: TGA and DTA curves of  $[\text{Hg}_2(\text{MSod})\text{Cl}_3(\text{H}_2\text{O})_7]\cdot\text{H}_2\text{O}$  Complex



Scheme 4: Thermal decomposition of  $[\text{Hg}_2(\text{MSod})\text{Cl}_3(\text{H}_2\text{O})_7]\cdot\text{H}_2\text{O}$  Complex

Table 6: DTA analysis of montelukast sodium and their simple metal complexes.

Compounds	Type	Tm (K)	E <sub>a</sub> (kJ mol <sup>-1</sup> )	n	α <sub>m</sub>	ΔS <sup>#</sup> (kJ K <sup>-1</sup> mol <sup>-1</sup> )	ΔH <sup>#</sup> (kJ mol <sup>-1</sup> )	Z S <sup>-1</sup>	Temp. (°C) TGA	Wt. Loss %		Assignment
										Calc	Found	
Montelukast Sodium	Endo	401	13.20	1.57	0.55	-0.31	-125.32	0.004	29.6 - 335.5	15.83	15.87	Elimination of 2HCl, and 2C <sub>3</sub> H <sub>7</sub> OH
	Exo	629	208.02	1.45	0.56	-0.30	-186.86	0.040	335.5-500	37.08	36.52	Loss of 2C <sub>3</sub> H <sub>7</sub> SH, C <sub>2</sub> H <sub>6</sub> , 2H <sub>2</sub> , 2C <sub>9</sub> H <sub>7</sub> N
	Exo	821	85.94	1.22	0.60	-0.31	-253.57	0.013	500-598	17.83	18.74	Decomposition of the rest ligand and formation of Na <sub>2</sub> O+24C
										29.25	28.78	Residue (Na <sub>2</sub> O+24C)
[Mn <sub>2</sub> (MSod) Cl <sub>3</sub> (H <sub>2</sub> O) <sub>3</sub> ].H <sub>2</sub> O	Endo	413.4	14.38	1.13	0.61	-0.31	-129.11	0.004	29.8 - 262.5	45.25	45.42	Dehydration of 4H <sub>2</sub> O and loss of 4 HCl, C <sub>3</sub> H <sub>7</sub> OH, C <sub>3</sub> H <sub>7</sub> S H <sub>2</sub> C <sub>3</sub> H <sub>4</sub>
	Exo	722	25.79	1.12	0.60	-0.31	-228.67	0.004	262.5-598.8	26.49	26.10	Decomposition of the rest ligand and formation of 2MnO+9C.
										28.24	28.60	Residue(2MnO+9C)
Co <sub>2</sub> (MSod) Cl <sub>3</sub> (H <sub>2</sub> O) <sub>3</sub> ].H <sub>2</sub> O	Endo	367.9	17.95	1.50	0.55	-0.31	-113.51	0.006	35.6 - 236.5	31.16	31.54	Dehydration of 4H <sub>2</sub> O, loss of 4HCl and C <sub>3</sub> H <sub>7</sub> OH
	Exo	603	47.45	1.40	0.57	-0.31	-186.12	0.009	236.5-400	4.34	4.54	Loss of C <sub>3</sub> H <sub>4</sub>
	Exo	736.6	93.70	1.38	0.57	-0.31	-225.65	0.015	400-586.6	23.18	22.35	Decomposition of the rest ligand and formation of 2CoO+18C
										41.30	41.51	Residue( 2CoO+18 C)
Cu <sub>2</sub> (MSod) Cl <sub>3</sub> (H <sub>2</sub> O) <sub>7</sub> ].H <sub>2</sub> O	Endo	392.9	18.60	1.56	0.55	-0.31	-121.54	0.006	34.4- 312.3	35.15	36.35	Dehydration of 8H <sub>2</sub> O, loss of C <sub>3</sub> H <sub>7</sub> OH 4HCl
	Exo	685.6	37.87	1.43	0.56	-0.31	-214.40	0.007	312.3 -573	13.93	13.42	Decomposition of the rest ligand and formation of 2CuO +27 C
										50.90	50.17	Residue(2CuO +27 C)

Complexes	Type	T <sub>m</sub> (K)	E <sub>a</sub> kJ mol <sup>-1</sup>	n	α <sub>m</sub>	ΔS <sup>#</sup> kJ K <sup>-1</sup> mol <sup>-1</sup>	ΔH <sup>#</sup> kJ mol <sup>-1</sup>	Z S <sup>-1</sup>	Temp. (°C) TGA	Wt. Loss %		Assignment
										Calc	Found	
Zn <sub>2</sub> ( (MSod) Cl <sub>3</sub> (H <sub>2</sub> O) <sub>7</sub> ]. H <sub>2</sub> O	Endo	473.8	11.40	1.22	0.60	-0.32	-149.96	0.003	38.1- 340.7	29.49	30.08	Dehydration of 8H <sub>2</sub> O and loss of 4 HCl
	Endo	714.6	21.80	0.98	0.64	-0.32	-227.21	0.004	340.7 -466.7	13.76	14.07	Loss of C <sub>3</sub> H <sub>7</sub> OH and C <sub>3</sub> H <sub>7</sub> SH
	Exo	818.2	270.06	1.24	0.59	-0.30	-244.87	0.040	466.7 -598.8	26.66	25.35	Decomposition of the rest ligand and formation of 2ZnO +11C
										30.07	30.53	Residue (2ZnO +11C)
[Hg <sub>2</sub> (MSod) Cl <sub>3</sub> (H <sub>2</sub> O) <sub>7</sub> ]. H <sub>2</sub> O	Endo	379.5	13.19	1.61	0.54	-0.31	-118.25	0.004	43.3-273.2	30.26	30.40	Dehydration of 8H <sub>2</sub> O, loss of C <sub>3</sub> H <sub>7</sub> OH 4 HCl, C <sub>2</sub> H <sub>2</sub>
	Exo	645	66.35	1.28	0.59	-0.31	-198.01	0.012	273.2 -513	69.64	69.63	Sublimation of 2Hg and decomposition of the rest ligand with no residue
	Exo	760.7	98.23	1.31	0.59	-0.31	-233.14	0.015				

## Conclusion

It was concluded that synthesis, characterization, spectral, thermal analysis and biological activity of montelukast sodium and its metal complexes were found favorable and effective.

## Reference

- Aasa R (1970). Powder Line Shapes in the Electron Paramagnetic Resonance Spectra of High-Spin Ferric Complexes. *The Journal of Chemical Physics*, 52(8): 3919-3930.
- Abraham A and Pryce MHL (1951). Theory of the nuclear hyperfine structure of paramagnetic resonance spectra in crystals. *Proceedings of the Royal Society of London A*, 205(1080): p. 135-153.
- Al Saadi MM, Meo SA, Mustafa A, Shafi A and Tuwajri ASA (2011). Effect of montelukast on free radical production in whole blood and isolated human polymorphonuclear neutrophils (PMNs) in asthmatic children, *Saudi Pharmaceutical Journal*, 19: 215-220.
- AlOmari MM, Zoubi RM, Hasan EI, Khader TZ and Badwan AA (2007). Effect of light and heat on the stability of montelukast in solution and in its solid state. *J. pharm. and biomedical analysis*, 45(3): 465-471.
- Austen KF (2008). The cysteinylleukotrienes: where do they come from? What are they? Where are they going? *Nature immunology*, 9(2): 113.
- Barnum DW (1961). Electronic absorption spectra of acetylacetonato complexes II: Hückel LCAO-MO calculations for complexes with trivalent transition metal ions, *Journal of Inorganic and Nuclear Chemistry*. 22(4): 183-191.
- Boca R (2004). Zero-field splitting in metal complexes. *Coordination chemistry reviews*, 248(9-10): 757-815.
- Brown ME (1988). Thermogravimetry (TG), in *Introduction to Thermal Analysis*. Springer. p. 7-22.
- Canadas M, Lopez-Torres E, Martinez-Arias A, Mendiola MA and Sevilla MT (2000). Spectroscopic and electrochemical properties of nickel (II), iron (III) and cobalt (II) complexes with benzilbisthiosemicarbazone importance of working conditions and the metal salt used in the final complex. *Polyhedron*, 19(18-19): 2059-2068.
- Carlin RL and Baker MJ (1964). The nitrate group as

- a ligand in some amine oxide complexes. *Journal of the Chemical Society*, 1964: 5008-5014.
- Condon CU (1928). *Physical Review*, 1928 .32: p. 858-872.
- Grau M, England J, Torres Martin de Rosales R, Rzepa HS, White AJ and Britovsek GJ (2013). Coordination Equilibria Between Seven- and Five-coordinate Iron (II) Complexes. *Inorganic Chemistry*, 52(20): 11867-11874.
- Hoang T, Farkas R, Wells C, McClintock S and Di Maso M (2002). Application of pressurized liquid extraction technology to pharmaceutical solid dosage form analysis. *Journal of Chromatography A*, 968(1-2): 257-261.
- Howlader M, Islam M and Karim M (2000). Synthesis of some 16-membered macrocyclic complexes of chromium (III), manganese (II), iron (III), cobalt (II), nickel (II) and copper (II) containing a tetra oxooctaazacyclohexadecane ligand.
- Jorgensen CK (1962). Absorption spectra of transition group complexes of sulphur-containing ligands. *Journal of Inorganic and Nuclear Chemistry*, 24(12): 1571-1585.
- Kent Barefield E, Busch DH and Nelson SM (1968). Iron, cobalt, and nickel complexes having anomalous magnetic moments, *Quart. Rev.*, 22 (4): 457-498.
- Kerkeni A, Daami-Remadi M, Tarchoun N and Khedher MB (2007). In vitro assessment of the antifungal activity of several compost extracts obtained from composted animal manure mixtures. *International Journal of agricultural research*, 2(9): 786-794.
- Lee RH, Griswold E and Kleinberg J (1964). Studies on the stepwise controlled decomposition of 2, 2'-bipyridine complexes of cobalt (II) and nickel (II) chlorides. *Inorganic Chemistry*, 3(9): 1278-1283.
- Lever A (1968). Electronic spectra of some transition metal complexes: Derivation of Dq and B. *J. of Chem. Edu.*, 45(11): 711.
- Lines M (1971). Orbital angular momentum in the theory of paramagnetic clusters. *The J. Chemical Physics*, 55(6): 2977-2984.
- Masoud MS, Ali AE and Elasala GS (2015b). Synthesis, spectral, computational and thermal analysis studies of metallocefotaxime antibiotics. *Spectrochimica Acta Part A: Molecular and Biomolecular Spectroscopy*, 149: 363-377.
- Masoud MS, Ali AE, Ghareeb DA and Nasr NM (2015a). Structural, spectral and thermal analysis of some metallocephradines. *Journal of Molecular Structure*, 1099: 359-372.
- Masoud MS, El-Marghany A, Orabi A, Ali AE and Sayed R (2013). Spectral, coordination and thermal properties of 5-arylidene thiobarbituric acids. *Spectrochimica Acta Part A: Molecular and Biomolecular Spectroscopy*, 107: 179-187.
- Masoud MS, Hafez AM and Ali AE (1998). Electron paramagnetic resonance and magnetic behaviour of ethanolamine complexes. *Spectroscopy letters*, 31(5): 901-911.
- Masoud MS, Khalil EA, Ramadan AM, Gohar YM and Sweyllam A (2007). Spectral, electrical conductivity and biological activity properties of some new azopyrimidine derivatives and their complexes. *Spectrochim. Acta*, 67A: 667-677.
- Matejovic I (1993). Determination of carbon, hydrogen, and nitrogen in soils by automated elemental analysis (dry combustion method). *Communications in Soil Science and Plant Analysis*, 24(17-18): 2213-2222.
- Matsuse H and Kohno S (2014). Leukotriene receptor antagonists pranlukast and montelukast for treating asthma. *Expert opinion on pharmacoth.*, 15(3): 353-363.
- Nakamoto K (1986). *Infrared and Raman Spectra of Inorganic and Coordination compounds*, 4th edn., *John Wiley, New York*.
- Okumu A, DiMaso M and Löbenberg R (2008). "Dynamic dissolution testing to establish in vitro/in vivo correlations for montelukast sodium, a poorly soluble drug." *Pharmaceutical research*, 25(12): 2778-2785.
- Peters-Golden M and Henderson Jr WR (2007). "Leukotrienes." *New England Journal of Medicine*, 357(18): 1841-1854
- Price ER and Wasson JRJ (1974). Chemical assessment. *Journal of Inorganic and Nuclear Chemistry*, 36 (1): p. 67.
- Radhakrishna T, Narasaraju A, Ramakrishna M and Satyanarayana A (2003). Simultaneous determination of montelukast and loratadine by HPLC and derivative

- spectrophotometric methods. *Journal of pharmaceutical and Biomedical analysis*, 31(2): 359-368.
- Rani DS, Lakshmi PV and Jayatyagaraju V (1994). Structural elucidation of manganese (II), iron (III), cobalt (II), nickel (II), copper (II) and zinc (II) complexes of a new multidentatedihydrazinoquinoxaline derivative. *Transition Metal Chemistry*, 19(1): 75-77.
- Reinen D and Friebel C (1984).  $\text{Cu}^{2+}$  in 5-coordination: a case of a second-order Jahn-Teller effect. II:  $\text{CuCl}_5^{3-}$  and other  $\text{CuIII}_5$  complexes: trigonalbipyramid or square pyramid?, *Inorganic Chemistry*, 23(7): 791-798.
- Sreekanth A, Joseph M, Fun HK and Kurup MP (2006). Formation of manganese (II) complexes of substituted thiosemicarbazones derived from 2-benzoylpyridine: Structural and spectroscopic studies. *Polyhedron*, 25(6): 1408-1414.
- Storms W (2007). Update on montelukast and its role in the treatment of asthma, allergic rhinitis and exercise-induced bronchoconstriction. *Expert opinion on pharmacotherapy*, 8(13): 2173-2187.
- Vogel AI (1989). *A Text Book of Quantitative Inorganic Analysis*. Longmans, London.
- Vyazovkin S, Goryachko V and Lesnikovich, A (1992). An approach to the solution of the inverse kinetic problem in the case of complex processes. Part III. Parallel independent reactions. *Thermochimica acta*, 197(1): 41-51.
- Wei J, Chen S, Huang C, Guo W, Yang S, Feng B and Chu J (2018). The cysteinyl leukotriene receptor 1 (CysLT1R) antagonist montelukast suppresses matrix metalloproteinase-13 expression induced by lipopolysaccharide. *International immunopharmacology*, 55:193-197.

\*\*\*\*\*